JOURNAL OF MATERIALS PROCESSING TECHNOLOGY 204 (2008) 239–247

journal homepage: www.elsevier.com/locate/jmatprotec

# A mathematical model to characterize effect of silica content in the boiler fly ash on erosion behaviour of boiler grade steel

*S.K. Das*, K.M. Godiwalla, Shubha S. Hegde, S.P. Mehrotra, P.K. Dey*

*National Metallurgical Laboratory, Council of Scientific & Industrial Research, Jamshedpur 831007, India*

ARTICLE INFO

*Article history:*
Received 30 March 2007
Received in revised form
11 October 2007
Accepted 5 November 2007

*Keywords:*
Mathematical models
Erosion rate
Fly ash
Silica content
Tensile properties
Steel grades

ABSTRACT

Fly ash particles entrained in the flue gas of coal-fired boilers can cause serious erosion on the critical components along the flow path. Such erosion can significantly jeopardise operational life of the boiler. A first principle based theoretical model has been developed embodying the mechanisms of erosion involving cutting wear, plastic deformation wear and effect of temperature on erosion behaviour, to predict erosion rates of pertinent boiler grade steels. Various grades of steels commonly used in the fabrication of boiler components and published data pertaining to boiler fly ash has been used in modelling the phenomena. The model also provides a quantitative predictive framework to study the effect of percentage of silica content in the ash particles on the erosion potential. The erosion sensitivity of particle impact velocity, angle of impingement and variation of surface temperature of the substrate (steel) have also been studied as a function of silica content in the ash. The model has been implemented in a computer code to predict the erosion rates at room and elevated temperature for various grades of steels under different particle impact conditions. The model predictions have been found to be in good agreement with the published data. This investigation illustrated that any minor increase in silica level in the ash can considerably aggravate the erosion rates, signifying the fact that silica content in the ash plays a critical role in characterising erosion potential of fly ash.



## 1. Introduction

Coal-based thermal power plants all over the world face serious problems of handling and disposal of the ash produced. The high ash content (30–60%) of the coal in India makes these problems more complex. In Indian coal-fired power plants, erosion induced by fly ash has been a perennial problem. This has long-term techno-economic implications on the life cycle management of the power plant components.

It has been observed that in coal-fired power stations, about 20% of the ash produced in the boilers is deposited on the boiler walls, economisers, air-heaters and super-heater tubes. The ash particles collide with the surfaces of the boiler steel components and the material is eroded from the surface. In cases of severe erosion, the components get perforated prematurely. As a consequence, the components may fail once they lose their structural integrity. The resulting penalty is not only the cost of replacing the components but also the cost of stoppage of power production. It is, therefore, of industrial importance to be able to predict the rate of erosion of the coal-fired boiler components to evolve strategies for preventive maintenance or replacement of these components to

* *Corresponding author*. Tel.: +91 6572271709x14; fax: +91 6572270527.
E-mail address: skd@nmlindia.org (S.K. Das).
0924-0136/$ – see front matter © 2007 Elsevier B.V. All rights reserved.
doi:10.1016/j.jmatprotec.2007.11.055

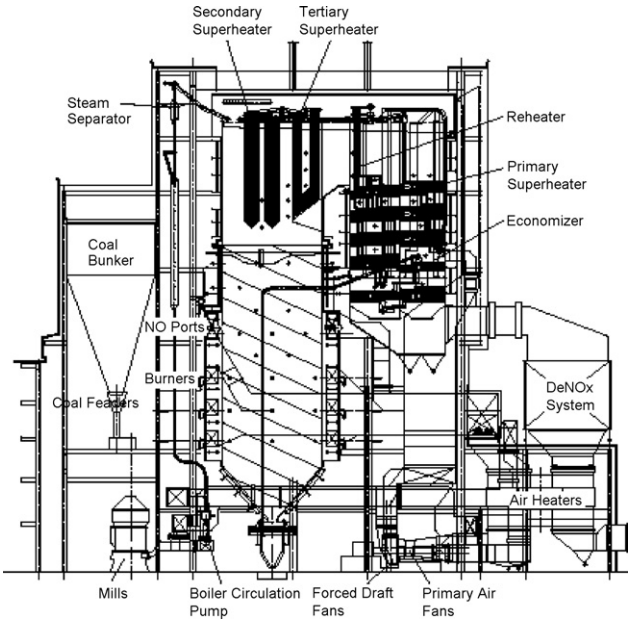


**Fig. 1 – Schematic of a coal-fired thermal power plant.**

avoid forced outages. Fig. 1 is a schematic of a coal-fired boiler assembly. Erosive wear of internal boiler tubes and other surfaces in the convective section of the furnace can also be of concern. Abrasive and erosive potential of the fly ash are function of several factors involving particle impact parameters and material parameters. The governing factors for severity of erosion are concentrations and size distributions of the harder constituents of the ash (mainly silica). Ash-free coal would not cause significant abrasion or erosion in coal plant; the wear damage is caused chiefly by the mineral impurities in coal.

The two most important constituents of fly ash are, silica ($SiO_2$) and alumina ($Al_2O_3$). It has been observed that "free" crystalline alumina mineral is hard and highly abrasive (Raask, 1985). However, in the majority of pulverized coal ashes alumina is present in a softer "combined" form of alumino-silicate glass with some mullite needles dispersed in the glassy matrix. Various investigators have addressed the issue of solid particle erosion and its quantification at room and elevated temperature. Many parameters are now known to influence erosion behaviour. The magnitude and direction of a particle's impact and rebounding velocity depend upon the conditions at impact and the particle-surface material combination. Grant and Tabakoff (1975) developed empirical correlation of the velocity restitution coefficients for sand particles impacting 410 stainless steel. Meng and Ludema (1995) have reviewed some of the erosion models that have been developed since Finnie (1960) proposed the first analytical erosion model. These models include a variety of parameters that influence the amount of material eroded from a target surface and the mechanism of erosion.

Bitter (1963) estimates total erosion rate, which is sum of erosion due to cutting mechanism and deformation mechanism without the effect of temperature by the following equations:

$$\varepsilon_{vT} = \varepsilon_{vD} + \varepsilon_{vC} \tag{1}$$

$$\varepsilon_{vD} = \frac{1}{2}\frac{M(V\sin\alpha - K)^2}{\delta} \tag{2}$$

$$\varepsilon_{vC1} = \frac{2MV(V\sin\alpha - K)^2}{(V\sin\alpha)^{1/2}}\left(V\cos\alpha - \frac{C(V\sin\alpha - K)^2}{(V\sin\alpha)^{1/2}}\chi\right) \quad \text{for } \alpha \geq \alpha_{p0} \tag{3}$$

$$\varepsilon_{vC2} = \frac{(1/2)\,M[V^2\cos^2\alpha - K_1(V\sin\alpha - K)^{3/2}]}{\chi} \quad \text{for } \alpha \leq \alpha_{p0} \tag{4}$$

where $\varepsilon_{vT}$ is total volume erosion rate, $\varepsilon_{vD}$ is the volume of material removed by deformation mechanism, $\varepsilon_{vC}$ is the volume of material removed by cutting mechanisms, $M$ is the total mass of impinging particle, $K$ is the velocity component normal to surface below which no erosion takes place in certain hard materials, $K_1$ is the proportionality constant, $C$ is the constant, $V$ is the velocity of particle, $p$ is the constant of plastic flow stress, and $\alpha$ is the impact angle.

The high-temperature erosion behaviour is associated with complex mechanism due to the variations in tensile properties, materials properties and interference of oxidation (Jun and Tabakoff, 1994; Fan et al., 1990; Tilly and Sage, 1970). It has been observed that erosion rate of steels impacted in the range of critical angles increases as the temperature of the steel is increased. Also, it is observed that the rates of erosion vary depending on the type and composition of steel. It is reported in the literature (Hutchings and Winter, 1974) that the effect of erosion mechanism of particle orientation during oblique impact of angular particles on lead and mild steel targets. It has been further reported by the investigators that for particle incidence angles close to 90°, erosion occurred by repeated plastic deformation of the target. Levy (1996) carried out experimental investigations on eroded metal surfaces using scanning electron microscopy at high magnifications. He observed that the loss of material from an eroded metal surface occurred by a combined cutting wear and extrusion-forging mechanism.

The ever-increasing capability of computers has led to the development of several numerical models for gas-particle flows. Tu et al. (1997a) carried out multidimensional computational fluid dynamics (CFD) simulations of flue gas with fly ash to predict erosion of the economisers in coal-fired boilers and subsequently Lee et al. (1999) used the Lagrangian approach while carrying out CFD simulations to predict erosion by fly ash of boiler tubes. The erosion behaviour of impacted fly ash particles on coal-fired boiler components has been studied at elevated temperature to characterize the erosion rate (mg of steel eroded/kg of erodent) as a function of various operating parameters (Das et al., 2006a,b,c).

It is difficult to specify the values of the velocity restitution coefficients for ash particles bouncing off the surface of a steel plate because, after an incubation period, the target material becomes pitted with craters and then after a slightly longer period, a regular ripple pattern forms on the eroded surface. Thus, the local impact angle between an ash particle and eroded surface may deviate considerably from the average. Furthermore, the particles themselves are irregular

in shape with several sharp corners. As the particles approach the target surface, their orientation is random. Thus, some particles strike a surface do very little work on the target material. On the other hand, other particles impact with a corner orientation in a manner similar to that of a cutting tool.

Silica is known to be highly abrasive and its quantity in the fly ash is of critical consequence on the solid particle erosion potential. Indian coals typically have ash content of 30–60%, which results in low calorific value. However, these coals are low in sulphur and heavy metals content. The experimental and theoretical investigations addressing characterization of erosion behaviour of fly ash on different boiler grade steel with varying degree of silica content is scanty in the available literature. A model has been formulated (Mbabazi et al., 2004) embodying composite mechanism of both cutting wear and plastic deformation to predict the erosion rate as a function of particle velocity, impingement angle, density of the target material and its tensile properties. The model has been extended to incorporate thermal effects on the solid particle erosion behaviour at elevated temperature (Das et al., 2006a,b,c). Sensitivity of silica content in the ash on the erosion rate has been investigated for various boiler grade steels at room and elevated temperature. An erosion index (Mbabazi et al., 2004) has been appropriately customised and employed to relate variation of the erosion rate with silica content.

## 2. Mathematical erosion model

Solid particle erosion is a process by which material is removed from various engineering components made of different metallic materials impacted by a stream of abrasive particles. The erosive wear is quantified by the volume or mass of the material that is removed by the action of the impinging particles as a function of impact parameter. It has been established from the earlier studies that there are three important phenomena by which metal can be removed at elevated temperature by the process of erosion (Hutchings and Winter, 1974; Mbabazi et al., 2004). The primary mechanisms of erosive wear are, erosion due to cutting wear (micro-machining action), repeated plastic deformation wear and weakening of tensile properties of the steel component at elevated temperature. The erosion at room temperature is due to cutting wear and plastic deformation. At elevated temperature, these mechanisms are further accentuated by the effect of temperature on tensile properties resulting in higher material loss. In general, erosion rate is a function of ash particle velocity, ash particle impingement angle, density of ash particle, density of target material yield stress of steel component and temperature of target material. In addition, silica content of the fly ash is also a critical parameter significantly influencing the erosive power of the impinging particle. The grades of steel considered in the present numerical investigation are, namely, carbon steel, 1.25Cr–1Mo–V steel and alloy steel 800.

### 2.1. Cutting wear

When an ash particle strikes the target material surface at an acute angle and a higher velocity than the critical velocity needed for the penetration of the surface of the material, which results in removal of some of the material. This process of removal of material is similar to the cutting action of a machine tool. At the impact point, the particle loses a fraction of its kinetic energy to the target material in the form of heat and energy for deformation of the surface. Very high levels of shear strain may be induced in the material at this point. When the shear strain exceeds the elastic strain limit of the target material, the particle penetrates and ploughs through the surface, thus, removing material.

It is assumed that the stresses acting at the contact point are constant during the wear process. The ash particle penetrating the surface of the material has to overcome the material's resistance to deformation. The dynamical equation representing the depth of penetration, $h$, of a particle of mass $m_p$ and diameter $d_p$, as it penetrates through the surface of a material is given by the following differential equation (Mbabazi et al., 2004):

$$m_p \frac{d^2h}{dt^2} = -\pi \frac{d_p}{2} hc\sigma_y \tag{5}$$

where $t$ is the time, $\sigma_y$ is the yield stress of the target material, $c$ is a particle shape factor equal to 3 for a sphere and $m_p = (1/6)\rho_p \pi d_p^3$.

Considering a spherical particle, Eq. (5) is integrated using the initial condition that at $t = 0$ $(dh/dt) = V \sin\beta$, and the following equation is obtained:

$$\frac{dh}{dt} = \pm\sqrt{V^2 \sin^2\beta - \frac{9\sigma_y h^2}{\rho_p d_p^2}} \tag{6}$$

where $V$ is the velocity, $\rho_p$ is the density of particle and $\beta$ is the angle of incidence. The physical significance of plus sign in Eq. (6) corresponds to an increase in the depth of penetration and the minus sign corresponds to a decrease in the depth of penetration. The maximum depth of penetration, $h_{max}$, occurs when $(dh/dt) = 0$, and is given by the following equation:

$$h_{max}^3 = \frac{d_p^3}{3^3} V^3 \sin^3\beta \left(\frac{\rho_p}{\rho_y}\right)^{3/2} \tag{7}$$

Since the volume of material that is cut away from the target surface by the impacting particle is proportional to $h_{max}^3$, the mass of material removed by a single particle is also proportional to the value of $h_{max}^3$. The mass of material eroded by cutting mechanism ($m_c$) by a single impacting particle, thus, may be given by the following equation:

$$m_c = K_c \rho_m h_{max}^3 = \frac{K_c \rho_m \rho_p^{3/2} d_p^3 V^3 \sin^3\beta}{3^3 \sigma_y^{3/2}} \tag{8}$$

here $K_c$ is a constant and $\rho_m$ is the density of target material. The erosion rate due to cutting wear, defined as the ratio of the mass of the material eroded from the target surface to mass of the impacting particle, is

$$\varepsilon_c = \frac{m_c}{m_p} = \frac{K_c \rho_m \rho_p^{3/2} d_p^3 V^3 \sin^3\beta}{3^3 \sigma_y^{3/2} (\pi \rho_p d_p^3/6)} = \frac{K_1 \rho_m \rho_p^{1/2} V^3 \sin^3\beta}{\sigma_y^{3/2}} \tag{9}$$

where $K_1$ is a constant.

### 2.2. Plastic deformation wear

During particle impact, the loss of material from an eroding metal surface is attributed to a combined extrusion-forging mechanism. Platelets are initially extruded from shallow craters made by the impacting particle. The high strain rates results in adiabatic shear heating in the surface region immediate to the impact site. A work-hardened zone forms beneath the immediate surface region. This is because, the kinetic energy of the impacting particles is sufficient to result in a considerably greater force being imparted to the metal than is required to generate platelets on the surface. The work-hardened zone reaches its stable hardness and thickness, which leads to steady-state erosion once the surface, is completely converted to platelets and craters. The reason that the steady-state erosion rate is the highest rate is that the subsurface cold-worked zone acts as an anvil, thereby increasing the efficiency of the impacting particles to extrude-forge platelets in the now highly strained and most deformable surface region. This cross-section of material moves down through the metal as erosion loss occurs. In the platelet mechanism of erosion, there is a localised sequential extrusion and forging of metal in a ductile manner, leading to removal of the micro-segments thus formed.

During plastic deformation, the normal component of the particle's kinetic energy is used to extrude-forge the material. The normal component of the kinetic energy of the particle is given by (Mbabazi et al., 2004):

$$E_1 = \frac{1}{2}\frac{\pi d_p^3}{6}\rho_p V^2 \sin^2\beta = \frac{\pi}{12}\rho_p d_p^3 V^2 \sin^2\beta \tag{10}$$

where $d_p$ and $\rho_p$ are the particle diameter and density, respectively, and $V$ and $\beta$ are the particle incident velocity and angle, respectively.

The work done by the normal force $N$ of the indenting particle in a direction normal to the surface from the time of surface contact until penetration stops at a depth $h_{max}$ is given by (Tu et al., 1997b):

$$E_2 = \int_0^{h_{max}} N dh \tag{11}$$

Sheldon and Kanhere (1972) formulated the following equation relating the force $N$ and the diameter $\delta$ of the crater formed in the indented surface:

$$N = a\delta^n \tag{12}$$

where constants, $n$ and $a$, are given as follows:

$$n = 2.0 \quad \text{and} \quad a = \tfrac{1}{4}\pi H_V$$

$H_V$ is Vickers hardness number of the target surface eroded by particle impingement. Substituting Eq. (12) into Eq. (11) yields

$$E_2 = \frac{\pi H_V}{4}\int_0^{h_{max}} \delta^2\, dh \tag{13}$$

The depth of penetration, $h$, is related to the instantaneous crater diameter $\delta$ and the particle diameter $d_p$ as

$$h = \tfrac{1}{2}(d_p - (d_p^2 - \delta^2)^{1/2}) \tag{14}$$

Eq. (14) is used to express the particle's depth of penetration in terms of the instantaneous crater diameter. Eq. (13) may be integrated with respect to the instantaneous crater diameter. Equating the work done during indention to the normal component of kinetic energy given in Eq. (10), the following equation is obtained:

$$\frac{\pi}{12} d_p^3 \rho_p V^2 \sin^2\beta = \frac{\pi H_V}{8}\int_0^{h_{max}} \frac{\delta^2\, d\delta}{(d_p^2 - \delta^2)^{1/2}} \tag{15}$$

The integral in Eq. (17), is evaluated and the maximum depth of penetration is derived as

$$h_{max}^3 = \frac{d_p^3 V^3 \sin^3\beta \rho_p^{3/2}}{H_V^{3/2}} \tag{16}$$

Since the dimensions of the crater formed by the impacting particle are all proportional to $h_{max}^3$, and since the amount of material removed is nearly the full crater size, the mass of material removed by a single particle is proportional to the value of $h_{max}^3$ derived in Eq. (16). The mass of material removed '$m_d$' by plastic deformation mechanism by a single particle is given by the following equation:

$$m_d = K_p \rho_m h_{max}^3 = K_p \rho_m \rho_p^{1/2} \frac{d_p^3 V^3 \sin^3\beta}{H_V^{3/2}} \tag{17}$$

where $K_p$ is a constant and $\rho_m$ is the density of the target material. The erosion rate, $\varepsilon_p$, due to plastic deformation is given by the following equation:

$$\varepsilon_p = \frac{m_d}{m_p} = \frac{K_p \rho_m \rho_p^{1/2} d_p^3 V^3 \sin^3\beta}{H_V^{3/2}(\rho_p \pi d_p^3/6)} = \frac{K_2 \rho_m \rho_p^{1/2} V^3 \sin^3\beta}{H_V^{3/2}} \tag{18}$$

where $K_2$ is a constant.

### 2.3. Erosion rate at elevated temperature

The erosion by fly ash on steel surfaces comprises of erosive wear due to the cutting mechanism and repeated plastic deformation mechanism. However, it is difficult to predict accurately the separate contributions by each of the two mechanisms to the overall material loss. Eq. (18), which was derived for the plastic deformation wear, is similar to Eq. (9) for the cutting wear. The yield stress of a metal can be related to the metal's hardness. The empirical relationship between the yield stress and Vickers hardness number is given by (Sheldon and Kanhere, 1972):

$$H_V = 2.7\sigma(T)_y \tag{19}$$

The overall erosion rate, combining the cutting and plastic deformation wear mechanisms, is given as

$$\varepsilon = \frac{K_3 \rho_m \rho_p^{1/2} V^3 \sin^3 \beta}{\sigma(T)_y^{3/2}} \quad (20)$$

where $K_3$ is a constant which is documented in the literature (Meng and Ludema, 1995; Jun and Tabakoff, 1994; Fan et al., 1990; Tu et al., 1997b). From the investigations carried out by various investigators (Fan et al., 1990; Sheldon and Kanhere, 1972; Sheldon et al., 1977; Shida and Fujikawa, 1985), the erosion rate due to solid particle impact depends upon the particle impingement angle and the characteristics of the particle-wall combination for modelling erosion by fly ash of ductile metal surfaces. The constant $K_3$ in Eq. (20) may be replaced by the particle erosion index giving the expression for the overall erosion rate

$$\varepsilon = \frac{K_e I_e(\mathrm{Si}) \rho_m \rho_p^{1/2} V^3 \sin^3 \beta}{\sigma(T)_y^{3/2}} \quad (21)$$

where $K_e$ is a constant, Si is the mass fraction of silica contained in the ash sample and $I_e$ is the erosion index of the ash, which relates the variation of the erosion rate to the silica content.

$$I_e = \alpha(\mathrm{Si})^{\beta} \quad (22)$$

where $\alpha$ and $\beta$ are coefficient related coal characteristics. The values of $\alpha \approx 3.5$ and $\beta \approx 4.95$.

Substituting Eq. (22) in Eq. (21), the expression for overall erosion rate is given as

$$\varepsilon = \frac{K_e \alpha(\mathrm{Si})^{\beta} \rho_m \rho_p^{1/2} V^3 \sin^3 \beta}{\sigma(T)_y^{3/2}} \quad (23)$$

The effect of temperature on the erosion behaviour of boiler components is of practical importance and an attempt was made to functionally correlate the tensile properties of these materials at elevated temperatures, which has been incorporated in the model. In the present model, the following process and materials parameters are considered for predicting erosion rate in the boiler components. The yield stress (kgf/mm$^2$) and temperature (K) functionality has been derived through a polynomial approximation for various grades of steel on the basis of the available tensile property (Shida and Fujikawa, 1985). The following expressions have been generated. The polynomial approximations to represent functionalities between the yield stress and temperature for various grades of steel are highly accurate and have a goodness of fit of 99.99%.

- Carbon steel

$$\sigma_y = 2 \times 10^{-5} T^2 - 0.0353T + 30.871 \quad (24)$$

- Cr–1Mo–V steel

$$\sigma_y = -2 \times 10^{-5} T^2 - 0.0278T + 48.703 \quad (25)$$

**Table 1 – Chemical composition of Indian fly ash (Basak and Bhattacharjee, 1989)**

| Constituent | Percentage range (%) |
|---|---|
| Silica ($SiO_2$) | 49–70 |
| Alumina ($Al_2O_3$) | 17–28 |
| Iron oxide ($Fe_2O_3$) | 5–10 |
| Calcium oxide (CaO) | 1–4 |
| Magnesium oxide (MgO) | 0.2–2 |
| Sulphur ($SO_3$) | 0.1–2 |
| Sodium oxide ($Na_2O$) + potassium oxide ($K_2O$) + manganese oxide (MnO) | 0.5–3 |

**Table 2 – Physico-chemical properties of Indian fly ash (Mukherjee and Borthakur, 2003)**

| Parameters | Range |
|---|---|
| Colour | Grayish |
| Bulk density (kg/m$^3$) | 960–1500 |
| Porosity (%) | 30–55 |
| Water holding capacity (%) | 35–55 |
| Sand (%) | 60–80 |
| Silt (%) | 10–35 |
| Clay (%) | 0.5–15 |
| Specific surface area (m$^2$/g) | 0.1038–2.4076 |
| pH | 3.5–12.5 |
| Electrical conductivity (dS/m) | 0.075–1.0 |

- 2.25Cr–1Mo steel

$$\sigma_y = -5 \times 10^{-8} T^3 + 10^{-5} T^2 - 0.0133T + 33.324 \quad (26)$$

- 12Cr–1Mo–V steel

$$\sigma_y = -5 \times 10^{-7} T^3 + 0.0005T^2 - 0.1379T + 59.169 \quad (27)$$

- 304 steel

$$\sigma_y = -2 \times 10^{-8} T^3 + 6 \times 10^{-5} T^2 - 0.0485T + 28.179 \quad (28)$$

- Alloy (Incoloy) 800

$$\sigma_y = -5 \times 10^{-8} T^3 + 7 \times 10^{-5} T^2 - 0.036T + 20.858 \quad (29)$$

Tables 1–3 show the chemical composition, physico-chemical properties and the chemical properties, respectively,

**Table 3 – Chemical properties of Indian fly ash (Mukherjee and Borthakur, 2003)**

| Parameters | Fly ash range (%) |
|---|---|
| Aluminum (Al) | 15.167–20.45 |
| Calcium (Ca) | 0.37–0.76 |
| Iron (Fe) | 4.447–6.562 |
| Manganese (Mn) | 0.002–0.84 |
| Magnesium (Mg) | 0.02–0.9 |
| Phosphorous (P) | 0.06–0.3 |
| Potassium (K) | 0.14–1.8 |
| Silicon (Si) | 27.413–29.554 |
| Sodium (Na) | 0.07–0.71 |
| Sulphur (S) | 0.03–0.055 |

**Table 4 – Chemical composition of various grades of steel (Shida and Fujikawa, 1985)**

| Steel | Amount (wt%) of the following metals | | | | | | |
|---|---|---|---|---|---|---|---|
| | C | Si | Mn | Ni | Cr | Mo | V |
| Carbon steel | 0.22 | 0.28 | 0.65 | | | | |
| 1.25Cr–1Mo–V | 0.13 | 0.25 | 0.55 | | 1.20 | 0.95 | 0.30 |
| 2.25Cr–1Mo | 0.10 | 0.34 | 0.44 | | 2.20 | 0.98 | |
| 12Cr–1Mo–V | 0.19 | 0.33 | 0.59 | | 11.40 | 0.87 | 0.28 |
| 304 | 0.08 | 0.62 | 1.68 | 10.25 | 18.50 | | |
| Alloy 800 | 0.07 | 0.51 | 1.13 | 32.85 | 20.85 | | |

of Indian fly ash. Table 4 shows the composition of various grades of steel considered in this study.

The computer codes in C++ have been developed to solve pertinent equations embodying erosion mechanism of cutting wear and repeated plastic deformation. The overall erosion is estimated from the contributions of both the mechanisms of the wear. The code predicts the erosion rate in terms of the weight (mg) of the target material removed per weight (kg) of the impacting fly ash particle as a function of impact velocity, impact angle, density and silica content of the ash particle and density and yield stress of the target material. The erosion behaviour at elevated temperature has been incorporated through the derived functionality of the tensile property (yield stress) with temperature using Eqs. (24)–(29) with appropriate modification of yield strength.

## 3. Results and discussion

The basic wear mechanism of ash particle erosion is composite actions of cutting wear, repeated plastic deformation and deterioration of the tensile properties of the steel at elevated temperature. An increase in silica content enhances the hardness of the impinging ash particle. Therefore, it augments proportionate contribution of cutting mechanism to the overall erosion rate under given operating conditions. However, accurate quantification of proportionate contributions of each mechanism separately (i.e. cutting wear and repeated plastic deformation) is an arduous task both theoretically and experimentally. The prediction of erosion behaviour has been verified with the published literature. Fig. 2 depicts predicted values of variation of erosion rate with impact velocity, at impingement angle of 30°, silica content of 55% and room temperature for 1.25Cr–1Mo–V steel, which is compared with the published data (Mbabazi et al., 2004). It may be observed that there is a monotonic increase in erosion rate with increasing particle velocity in both prediction and measurement. Theoretical predictions are found to be in good agreement with the published data.

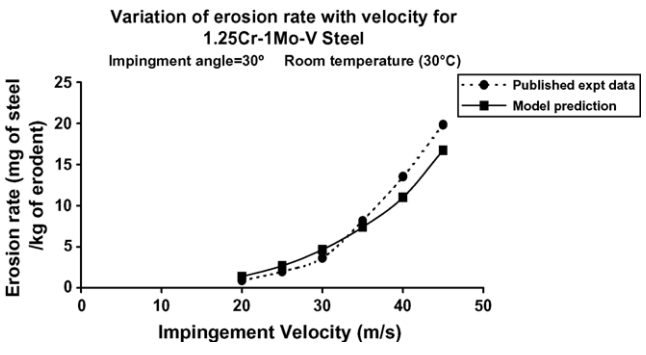


**Fig. 2 – Variation of erosion rate with impingement velocity (1.25Cr–1Mo–V steel).**

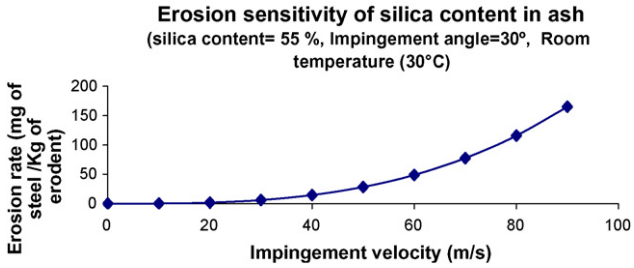


**Fig. 3 – Effect of silica content on the erosion rate (carbon steel) (silica content = 55%, impingement angle = 30°, at room temperature).**

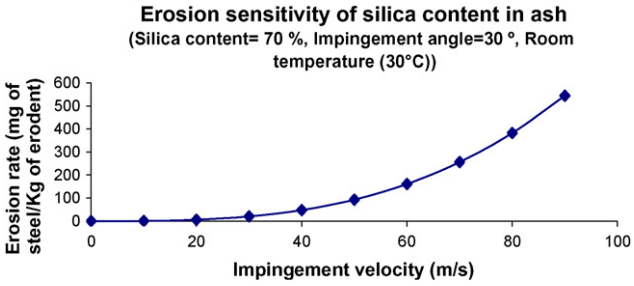


**Fig. 4 – Effect of silica content on the erosion rate (carbon steel) (silica content = 70%, impingement angle = 30° at room temperature).**

Figs. 3 and 4 show the erosion rate as a function of particle velocity for carbon steel with impingement angle 30° at room temperature (30 °C) with silica content 55% and 70% in the fly ash, respectively. From these figures, it may be observed that the erosion rate is about 47 mg/kg of erodent for 70% silica content in comparison to the silica content of 55% where the erosion rate is 14 mg/kg of erodent at an impact velocity of 40 m/s. This implies that an increase of about 15% in the silica content of the ash has a significant impact on the erosion rate, which has increased 235% approximately under similar particle impact conditions. It may further be observed from both these figures that the erosion rate depicts a nearly linear relationship with impingement velocity for lower values and increases at a faster rate for higher values. The overall erosion characteristic appears to follow a power law relationship

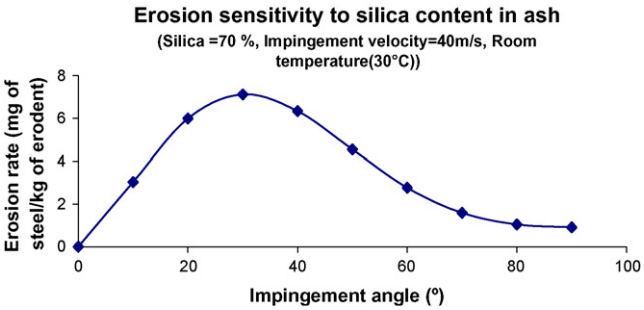


**Fig. 5 – Effect of silica content on the erosion rate (1.25Cr–1Mo–V steel) (silica content = 55%, impingement velocity = 40 m/s, at room temperature).**

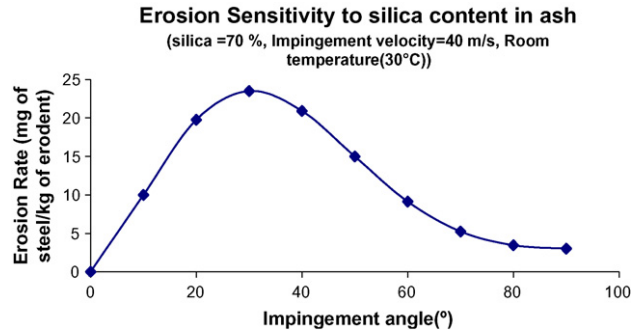


**Fig. 6 – Effect of silica content on the erosion rate (1.25Cr–1Mo–V steel) (silica content = 70%, impingement velocity = 40 m/s, at room temperature).**

(Das et al., 2006a; Mbabazi et al., 2004). This verifies the fact that the erosion behaviour predicted by the present model is consistent with regard to ductile materials.

Figs. 5 and 6 show the erosion rate as a function of impingement angle with silica content 55% and 70% in the fly ash, respectively, for 1.25Cr–1Mo–V steel at a particle impact velocity 40 m/s and room temperature. From these figures it may be observed that the erosion rate for 70% silica content is about 23 mg/kg of erodent in comparison to the silica content of 55% where the erosion rate is 7 mg/kg of erodent (say) at an impact angle of 30°. This indicate that an increase of about 15% in the silica content of the ash has a significant impact on the erosion rate, which has increased more than 200% under similar particle impact conditions. Fig. 7 shows

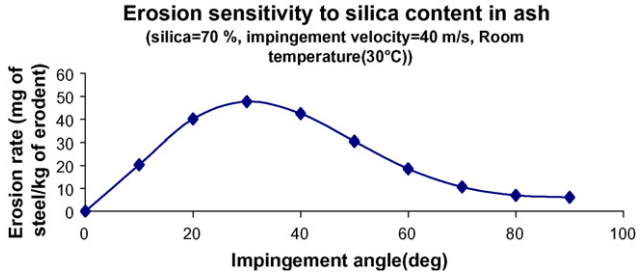


**Fig. 7 – Effect of silica content on the erosion rate (carbon steel) (silica content = 70%, impingement velocity = 40 m/s, at room temperature).**

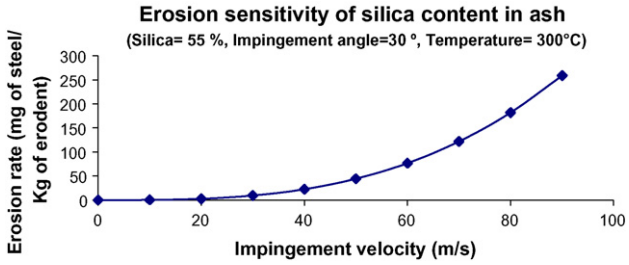


**Fig. 8 – Effect of silica content on the erosion rate (carbon steel) (silica content = 55%, impingement angle = 30°, temperature = 300 °C).**

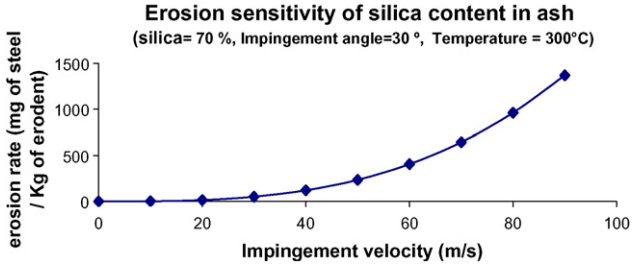


**Fig. 9 – Effect of silica content on the erosion rate (carbon steel) (silica content = 70%, impingement angle = 30°, temperature = 300 °C).**

the erosion rate as a function of impingement angle with silica content 70% in fly ash for carbon steel. In Figs. 6 and 7, erosion rates are found to be 23 mg/kg and 47 mg/kg for 1.25Cr–1Mo–V steel and carbon steel, respectively. This is attributed to the superior tensile properties and erosive wear resistant capability of 1.25Cr–1Mo–V steel in comparison to carbon steel. The range of critical impingement angle for extreme erosion rate is 20–40° and this is reflected in the above figures for various percentage of silica content in the ash. Figs. 8 and 9 show the erosion rate as a function of particle velocity with silica content 55% and 70% in the fly ash, respectively, for carbon steel with impingement angle 30° at elevated temperature (300 °C). From these Figs. 8 and 9 it may be observed that the erosion rate for 70% silica content is about 74 mg/kg of erodent in comparison to the silica content of 55% where the erosion rate is 22 mg/kg of erodent (say) at an impact velocity of 40 m/s. This implies the fact that an increase of about 15% in the silica content of the ash has a significant impact on the erosion rate, which has increased more than 200% under similar particle impact conditions. Figs. 10 and 11 illustrate the variation of erosion rate as a function of temperature for carbon steel target material with ash particle silica content of 55% and 70%, respectively. The computed results shown in these figures pertain to the ash particle velocity and impingement angle; 30 m/s and 30°, respectively. The results illustrate that the erosion rate increases monotonically with the increase in temperature. It is observed from these results that the erosion rate for 70% silica content in the ash particle (31 mg/kg of erodent) is significantly higher in comparison to the silica content 55% in the ash (9 mg/kg of erodent) at 300 °C. This implies that an increase of about 15% in the silica content of the ash has a

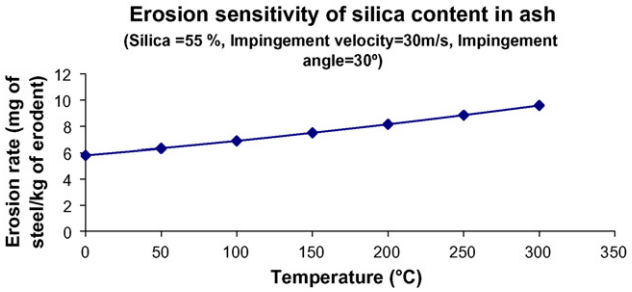


**Fig. 10 – Effect of silica content on the erosion rate (carbon steel) (silica content = 55%, impingement velocity = 30 m/s, impingement angle = 30°).**

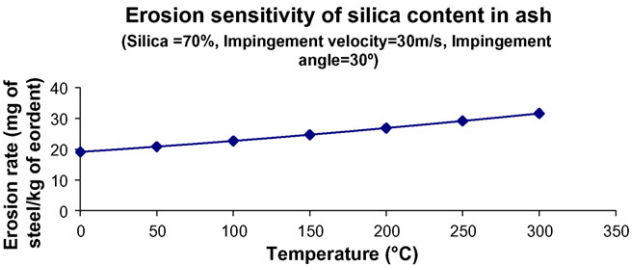


**Fig. 11 – Effect of silica content on the erosion rate (carbon steel) (silica content = 70%, impingement velocity = 30 m/s, impingement angle = 30°).**

significant impact on the erosion rate, which has increased more than 200% under identical particle impingement conditions. Figs. 12 and 13 show the variation of erosion rate as a function of increasing temperature of the target material for a typical ash particle with silica content of 55% and 70% for 1.25Cr–1Mo–V steel, respectively. The particle velocity and impingement angle considered are 30 m/s and 30° for depicted results as shown in Figs. 12 and 13. It may further be observed from these figures that the erosion rate for 70% silica content is about 14 mg/kg of erodent is more in comparison to the silica content 55% which is 4 mg/kg of erodent at 300 °C. This indicates that an increase of about 15% in the silica content of the ash has a significant impact on the erosion rate, which has augmented close to 250% under similar particle impact conditions. Fig. 14 shows the variation of erosion rate as a function of increasing temperature of the target material for a typical ash particle with silica content of 70% for steel grade alloy 800.

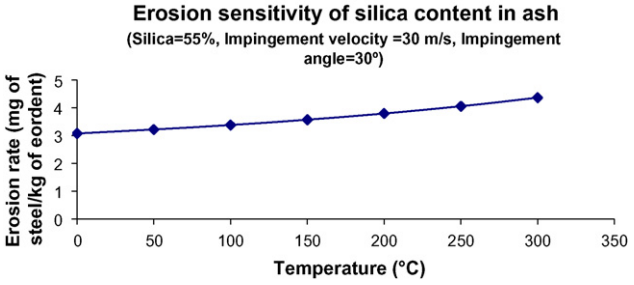


**Fig. 12 – Effect of silica content on the erosion rate (1.25Cr–1Mo–V steel) (silica content = 55%, impingement velocity = 30 m/s, impingement angle = 30°).**

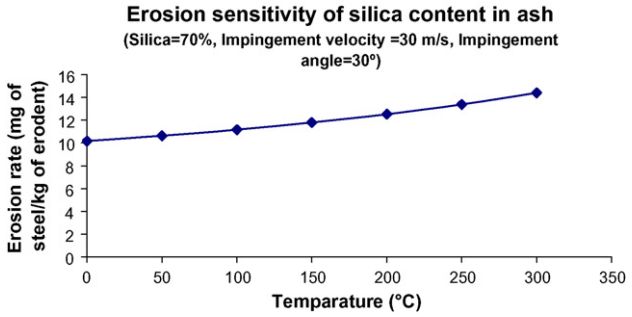


**Fig. 13 – Effect of silica content on the erosion rate (1.25Cr–1Mo–V steel) (silica content = 70%, impingement velocity = 30 m/s, impingement angle = 30°).**

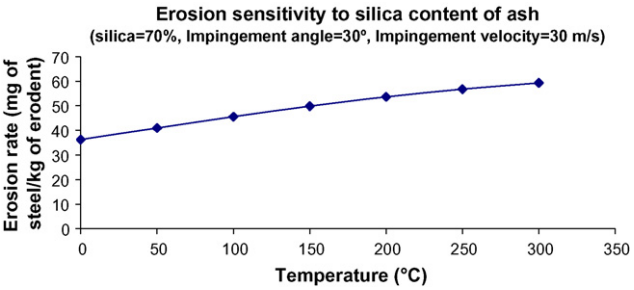


**Fig. 14 – Effect of silica content on the erosion rate (steel grade: alloy 800) (silica content = 70%, impingement velocity = 30 m/s, impingement angle = 30°).**

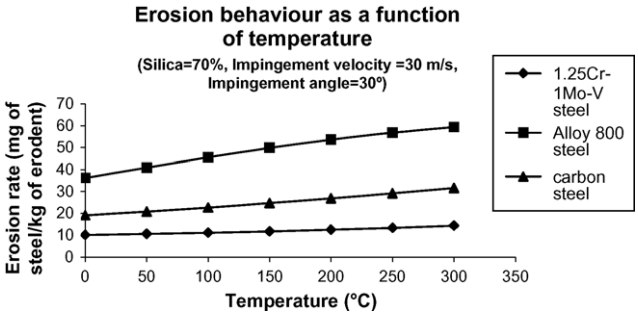


**Fig. 15 – Erosion behaviour for various grades of steel with temperature variation (silica content = 70%, impingement velocity = 30 m/s, impingement angle = 30°).**

The particle velocity and impingement angle considered are 30 m/s and 30° and the erosion rate is found to be 59 mg/kg of erodent with 70% of silica content in the ash. The erosion rate is found to be more for alloy steel 800 with respect to carbon steel and 1.25Cr–1Mo–V steel. This indicates that the erosion resistance of 1.25Cr–1Mo–V steel is the maximum and alloy steel 800 is minimum among these grades of steel. This is attributed to the superior tensile properties (yield strength and hardness) of carbon steel and 1.25Cr–1Mo–V steel with respect to alloy steel 800 at both room and elevated temperature.

The erosion behaviour of boiler grade steels, namely, carbon steel, 1.25Cr–1Mo–V steel and alloy steel 800 has been further analysed at elevated temperature. Fig. 15 shows the relative variation of erosion rate as a function of temperature for above grades of steel. For silica content of 70% in the ash,

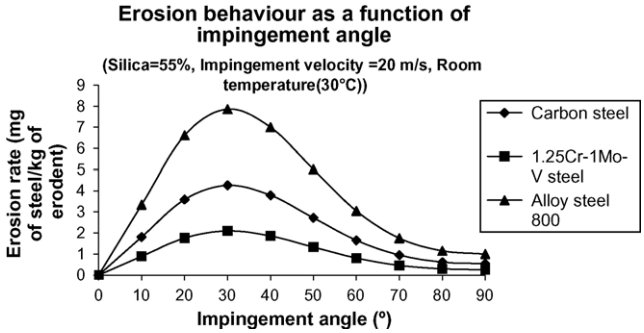


**Fig. 16 – Erosion behaviour for various grades of steel with angle variation (silica content = 55%, impingement velocity = 30 m/s, at room temperature).**

the erosion rate of alloy steel 800 is almost twice as high as carbon steel and almost close to four times that of 1.25Cr–1Mo–V steel. The rate of change of erosion rate with temperature ($d\varepsilon/dT$) is higher for alloy steel 800 in comparison to carbon steel. Further, $d\varepsilon/dT$ is also relatively higher for carbon steel in comparison to 1.25Cr–1Mo–V steel under identical impact conditions. Fig. 16 shows a relative variation of erosion rate as a function of impingement angle for the given steel grades. Erosion rate for alloy steel 800 is observed to be maximum with respect to other grades for silica content 55% and with impact velocity 20 m/s. The rate of change of erosion rate with impingement angle ($d\varepsilon/d\beta$) is sharper for alloy steel 800 with respect to other two grades of steel.

## 4. Conclusion

A model to predict the erosion rate for fly ash particle impingement on boiler component surfaces has been developed and the variation of erosion rate with various parameters investigated and found to be in good agreement with the published experimental data. Sensitivity of silica content in the ash on the erosion potential has also been studied for various boiler grade steels at room and elevated temperature. The erosion rate increases with increase in the impingement angle, with the maximum erosion rate occurring at an impingement angle of about 30°. Thereafter, the erosion rate decreases with further increase in the impingement angle. It is also noted that the erosion rate at low impingement angles increases significantly with increasing temperature but at high impingement angles the effect of temperature is insignificant. All the steel grades investigated in this study show an increase in erosion rate with temperature. The variation of erosion rate shows a monotonic rise with ash particle impact velocity. The code has been validated with the published information. The present modelling endeavour exemplifies that any minor increase in silica level in the ash can considerably aggravate the erosion rates. This is indicative of the phenomena that the silica content in the ash plays a vital role in evaluating erosion potential of fly ash. The influences of the shape and rotation angle of the ash particles with higher silica content on the erosion rate also need further investigation using appropriate mathematical models.

## REFERENCES


Basak, P.K., Bhattacharjee, P.K. (Eds.), 1989. Indian Coals, p. 8.

Bitter, J.G.A., 1963. A study of erosion phenomenon, Part 1. Wear 6, 5–21.

Das, S.K., Godiwala, K.M., Mehrotra, S.P., Dey, P.K., 2006a. Mathematical modeling of erosion behavior of impacted fly ash particles on coal fired boiler components at elevated temperature. High Temp. Mater. Process. 25, 323–335.

Das, S.K., Godiwala, K.M., Mehrotra, S.P., Sastry, K.K.M., Dey, P.K., 2006b. Analytical model for erosion behavior of impacted fly-ash particles on coal fired boiler components. Sadhana 31, 1–13.

Das, S.K., Godiwala, K.M., Hegde, S., Mehrotra, S.P., Dey, P.K., 2006c. A mathematical ductile erosion model to characterize ash particles erosion on boiler grade steel surfaces. In: International Conference on Industrial Tribology, ICIT-2006, November 30–December 02, IISc, Bangalore, India, pp. 189–196 (Conference volume).

Fan, J.D., Zhou, K.C., jin, J., 1990. Numerical prediction of tube row erosion by coal ash impaction. Chem. Eng. Commun. 95, 75–88.

Finnie, I., 1960. Erosion of surfaces by solid particles. Wear 142, 87–103.

Grant, G., Tabakoff, W., 1975. Erosion prediction in turbo machinery resulting from environmental solid particles. J. Aircraft 12, 471–478.

Hutchings, I.M., Winter, R.E., 1974. Particle erosion of ductile metals: a mechanism of material removal. Wear 27, 121–128.

Jun, Y.D., Tabakoff, W., 1994. Numerical simulation of a dilute particulate flow (laminar) over tube banks. Trans. ASME: J. Fluid Eng. 116, 770–777.

Lee, B.E., Fletcher, C.A.J., Behania, M., 1999. Computational prediction of tube erosion in coal fired power utility boilers. J. Eng. Gas Turb. Power 121, 746–750.

Levy, A.V., 1996. The platelet mechanism of erosion of ductile metals. Wear 180, 1–21.

Mbabazi, J.G., Sheer, T.J., Shandu, R., 2004. A model to predict erosion on mild steel surfaces impacted by boiler fly ash particles. Wear 257, 612–624.

Meng, H.C., Ludema, K.C., 1995. Wear models and predictive equations: their form and content. Wear 181–183, 443–457.

Mukherjee, S., Borthakur, P.C., 2003. Effects of alkali treatment on ash and sulphur removal from Assam coal. Fuel Process. Technol. 85, 93–101.

Raask, E., 1985. Mineral Impurities in Coal Combustion, Behavior: Problems, and Remedial Measures, second ed. Hemisphere Publishing Corporation, New York.

Sheldon, G.I., Kanhere, A., 1972. An investigation of impingement erosion using single particles. Wear 21, 195–209.

Sheldon, G.I., Maji, J., Crowe, C.T., 1977. Erosion of a tube by gas-particle flow. Trans. ASME: J. Eng. Mater. Technol. 99, 138–142.

Shida, Y., Fujikawa, H., 1985. Particle erosion behaviour of boiler tube materials at elevated temperature. Wear 103, 281–296.

Tilly, G.P., Sage, W., 1970. The interaction of particle and material behaviour in erosion processes. Wear 16, 447–465.

Tu, J.Y., Fletcher, C.A.J., Behnia, M., Reizes, J.A., Jones, P., 1997a. Prediction of flow and erosion in power utility boilers and comparison with measurement. J. Eng. Gas Turb. Power 119, 709–716.

Tu, J.Y., Fletcher, C.A.J., Behnia, M., Reizes, J.A., Owens, D., Jones, P., 1997b. Prediction of flow and erosion in power utility boilers and comparison with measurement. J. Eng. Gas Turb. Power 119, 709–716.